Compressibility and polymorphism of α-As_4S_4 realgar under high pressure

2009 J. Phys.: Condens. Matter 21 385401

(http://iopscience.iop.org/0953-8984/21/38/385401)

J. Phys.: Condens. Matter **21** (2009) 385401 (7pp) doi:10.1088/0953-8984/21/38/385401

Compressibility and polymorphism of α-As_4S_4 realgar under high pressure

M A Tuktabiev[1], S V Popova[1], V V Brazhkin[1], A G Lyapin[1] and Y Katayama[2]

[1] Institute for High Pressure Physics, Russian Academy of Sciences, 142190, Troitsk, Moscow region, Russia
[2] Japan Atomic Energy Agency (JAEA), SPring-8, 1-1-1 Kuoto, Sayo-cho, Sayo-gun, Hyogo 679-5143, Japan

Received 27 April 2009, in final form 9 July 2009
Published 24 August 2009
Online at stacks.iop.org/JPhysCM/21/385401

Abstract

The energy-dispersive x-ray diffraction technique has been employed to study the structure and equation of state of realgar As_4S_4 under pressures up to 8 GPa at room temperature. We have obtained pressure dependences of the unit cell parameters and volume for the monoclinic structure of realgar. An approximation of the equation of state through the Murnaghan equation gives the bulk modulus and its derivative, $B_0 = 8.1 \pm 0.5$ GPa and $B_0' = 9.0 \pm 0.5$, respectively. A comparison of the obtained values with the corresponding values for other molecular crystals is drawn and discussed. At a pressure of around 7 GPa, realgar showed a polymorph transition to a new molecular phase with a supposedly orthorhombic structure. Such identification is evidenced by the presence of geometrical correlations between the parameters of the parent monoclinic phase and those of the new phase, and the phase transition is likely to be associated with the removal of a monoclinic distortion in the unit cell.

(Some figures in this article are in colour only in the electronic version)

1. Introduction

Arsenic chalcogenides are of great interest for high pressure research. In the As–S system, both ordinary covalent As_2S_3 and inorganic molecular As_4S_4, As_4S_3 and other compounds are realized. These compounds are minerals of the Earth's upper mantle: crystals of orpiment As_2S_3 and realgar As_4S_4 are found at the Earth's surface in high seismicity areas. Chalcogenide glasses $As_{1-x}S_x$ are of particular interest in the context of their high infrared transparency, photostructural sensitivity and doping ability [1–4]. Recently, glasses of the realgar As_4S_4-like composition have been obtained under high pressures by quenching of the melt [5].

The investigation into the realgar structure and properties is essential since this mineral is formed at the boundary between the upper mantle and Earth's crust under pressures of 5–7 GPa. In addition, realgar is an interesting and rather rare example of a molecular inorganic crystal with closed globular molecules. The information on the equation of state of this crystal is of both fundamental and theoretical interest. The character of the molecule displacements in the lattice cell during compression may be a precursor of possible phase transitions. The bulk modulus value and its variation with pressure directly reflect the character of intermolecular forces. On the other hand, the data on the bulk modulus value is of vital importance in making a separation between the phonon-excitation (explicit term driven by phonon–phonon interactions) and volume-driven (implicit term driven by volume dilatation) contributions to the temperature derivatives of phonon frequencies, $\mathrm{d}\omega/\mathrm{d}T$ [6, 7]. In particular, the realgar phonon modes exhibit regular behavior: for external (intermolecular) modes, $\mathrm{d}\omega/\mathrm{d}T$ is dominated by the implicit effect; for internal (intramolecular) modes, it is dominated by the explicit effect [6]. However, the behavior of the Raman modes was analyzed in [6] merely on the basis of an empirical estimate of the As_4S_4 compressibility. This estimate was inexact, as will be shown in this work.

There are several modifications of crystalline arsenic monosulfide (As_4S_4), with four molecular polymorphs known with certainty. A great number of studies have been devoted to their crystalline structures and mutual transformation under the effect of temperature and light radiation. The ground state of As_4S_4 is realgar (α-As_4S_4) [8], in which the As_4S_4 molecules are bonded by van der Waals (molecular) forces. At

Table 1. Symmetry group, lattice parameters, and volume of the elementary cell for the polymorphs of As_4S_4.

Phase	Group	a (Å)	b (Å)	c (Å)	β (deg)	Volume (Å^3)	References
Realgar	$P2_1/n$	9.32	13.57	6.59	106.4	787.7	[8]
Pararealgar	$P2_1/n$	9.91	9.66	8.50	97.3	807.0	[15]
β-As_4S_4	$C2/c$	9.96	9.33	8.90	102.5	807.4	[16]
As_4S_4(II)	$P2_1/n$	11.19	10.00	7.15	92.8	799.2	[14]
χ-phase	$C2/c$	9.76	9.52	9.08	101.0	828.2	[12]

a temperature of 256 ± 5 °C under normal pressure, realgar transforms to the β-As_4S_4 phase, which melts at a temperature of 307 ± 5 °C [9]. The β-phase is metastable at room temperature. Another As_4S_4 modification, pararealgar, was described in [10]. Realgar and the β-phase were found to transform to pararealgar on exposure to light [11–13]. In doing so, this transition was always achieved through an intermediate so-called 'χ-phase' [11, 12] and preceded by an increase in the unit cell volume from 798 to 810 Å^3 for realgar and from 803 to 821 Å^3 for the β-phase [12]. In fact, the χ-phase represents a more disordered analog of the β-phase with an expanded unit cell [12]. However, the existence of the χ-phase as a pure molecular modification of As_4S_4 still seems questionable [13]. One more modification, As_4S_4(II), is obtained by quenching from the AsS melt at temperatures from 500 to 600 °C to room temperature [14]. All five phases mentioned above have monoclinic singony. The unit cell parameters for these phases are shown in table 1. It is reasonable that the lattice parameters of mineralogical samples of realgar vary from one sample to another (by ∼1%) due to the presence of defects and impurities [12]. Note that the structures of the first four polymorphs differ not only in molecular packing but also in the type of molecules. In realgar and the β-phase, the molecules are centrally symmetric (a S atom is bonded to two As atoms, and an As atom is bonded not only to two S atoms but also to one As atom), whereas in pararealgar and As_4S_4(II), neighbors of different As atoms in the molecule are different (one atom has 2As + S, two atoms have As + 2S and one more atom—3S) (see, for example, [12, 13]).

The pressure effect on the structure and properties of realgar is far less known. At the same time we are aware that both organic and inorganic molecular compounds can experience a variety of transformations, such as polymorphic transformations, which include polymerization, solid-phase amorphization and others. In [17], As_4S_4 was investigated under pressures of 4–7 GPa and temperatures of 420–1000 °C and two irreversible transitions were found with temperature changes at 420–500 °C and 800–1000 °C, respectively. X-ray diffraction patterns of the new phases were obtained but the structure of the phases was not determined.

In [18], an As_4S_4 phase diagram up to 5.5 GPa and 700 °C is presented. The diagram shows two high pressure phases. One phase exists in the range of 400–500 °C and 1.7–3.5 GPa, the other—at 500 °C starting from 2.5 GPa. As the pressure increases, the temperature stability range of the second phase extends upwards and downwards. The first phase was indexed in the orthorhombic singony with the parameters a = 12.22 Å, b = 11.17 Å, and c = 10.00 Å; its density was 3.64 g cm^{-3}. The structure of the second phase was not determined.

As an object for the present study, natural realgar of the Kamchatka Peninsular origin was taken. Using the energy-dispersive x-ray diffraction technique, the realgar structure and compressibility under pressure at room temperature, as well as its possible polymorphism, were examined.

2. Experimental details

Realgar, As_4S_4, of 99.7% chemical purity was used as a starting material. The *in situ* structural study of crystalline realgar was carried out by the energy-dispersive x-ray diffraction (EDXD) method in the SMAP-180 press machine at the BL14B1 beam-line of SPring-8. The As_4S_4 samples were placed in a container from either hexagonal BN or high-purity graphite. The cubic environment was made from a mixture of amorphous boron and epoxy resin. Cylinder-shaped samples were produced by pressing from a polycrystalline powder of 10–20 mkm in grain size. A cubic press was used for generating a high pressure of up to 8 GPa. The pressure was determined from the equation of state of NaCl. The uncertainty of pressure measurements using the NaCl pressure standard (basically it was determined by dispersion of the experimental reflection positions from the calculated ones) was 0.05 GPa for the majority of points, sometimes reaching 0.1 GPa.

During measurements, the energy-dispersive Canberra detector (the energy range for a white beam 5–150 keV) was kept at a fixed angle $2\theta = 6°$. The energy range E of the detection of scattered photons for the reflections from a particular realgar sample under pressure (with regard to the nonlinearity of the detector and a considerable decrease in the sensitivity of intensity at the edges of the energy range) was roughly 30–110 keV, which corresponded the scattering wavevector range Q ($Q = 2\pi/d$, where d is an interplanar space of diffraction) approximately from 1.6 to 5.6 Å^{-1}. Reflections for realgar were reliably detected and identified in the 1.8–4.8 Å^{-1} scattering wavevector range.

3. Results and discussion

Figure 1 displays an x-ray diffraction pattern taken with a standard diffractometer STOE STADI MP. The experimental diffraction pattern is in good agreement with tabular data from the PDF-2 (JCPDS-ICDD) database [19, 20]. Note that the more recent work [20] gives a more detailed picture of the reflection amplitudes for larger Q (smaller d). In this case, there are no noticeable impurities of other phases.

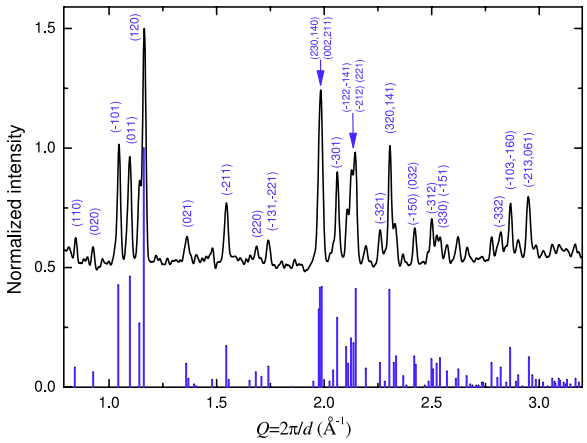

Figure 1. A normalized x-ray diffraction pattern (shifted by 0.5) of the initial realgar (Cu Kα, transmission geometry) in comparison with the stick pattern from [19]. The strongest reflections are indexed according to [19].

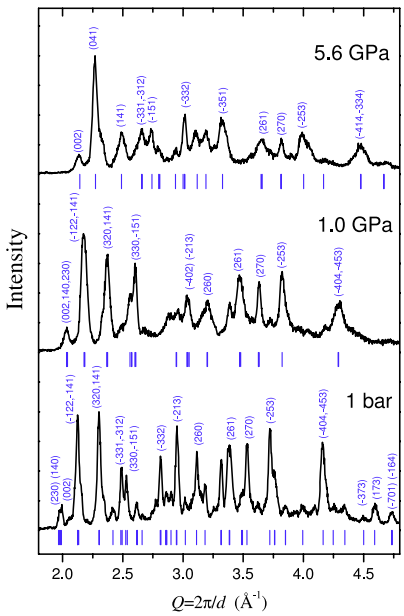

Figure 2. EDXD x-ray diffraction patterns from realgar at normal conditions and at two pressure points. The patterns are accompanied by the selected stick patterns. Several peaks on the patterns are not marked by sticks, but they still can be easily identified with corresponding *hkl* indices if we increase the accuracy criterion $\Delta(1/d^2)$ of identification by a factor ~2 (see also the text).

Experimental diffraction patterns for realgar under pressure are presented in figure 2. A diffraction pattern for normal conditions was obtained under the same experimental conditions, i.e., when the sample was confined within the experimental high pressure assembly in an unloaded press. Following the determination of the experimental positions of the reflections and by varying the unit cell parameters a, b, c and the angle β, the calculated positions of the reflections (h, k, l) were fitted to the experimental ones by the least-square method in the $1/d^2$ space. For the realgar monoclinic singony, this value is connected with the Miller indices

$$\frac{1}{d^2} = \frac{h^2}{a^2 \sin^2\beta} + \frac{k^2}{b^2} + \frac{l^2}{c^2 \sin^2\beta} - \frac{2hl\cos\beta}{ac\sin^2\beta}. \qquad (1)$$

In doing so, calculated reflections with large deviations from the experimental peak maxima were separated through several iterations, using a gradually reduced accuracy parameter $\Delta(1/d^2)$ as the criterion. Figure 2 shows the selected stick patterns with the accuracy criterion for a diffraction pattern under normal conditions $\Delta(1/d^2) = 0.001$ Å^{-2}, while under pressure, when the reflections broadened, $\Delta(1/d^2) = 0.002$ Å^{-2}. For these particular quantitative criteria not absolutely all weak experimental peaks in figure 2 are marked by sticks, but they still can be identified if we take into account the width of peaks. Naturally, at normal pressure the intensive peaks were referred to the tabular ones [20]. In figure 2, the key experimental diffraction peaks are indexed according to the selected stick patterns and you can see the evolution of some peak positions under pressure. Since the measurement step under pressure was regular and not wide, the identification of particular reflections, going from some pressure point to the next one, was for the most part of the diffraction pattern sufficiently valid and accurate.

The values obtained for the unit cell parameters of realgar are summarized in table 2. The experimental uncertainties in table 2 were calculated from the deviations between the calculated and experimental diffraction peak positions under an assumption that the relative uncertainties of all lattice

Table 2. Lattice parameters and volume of the elementary cell for realgar at different pressures. The uncertainties are presented in parentheses in the unit of the last symbol.

Pressure (GPa)	a (Å)	b (Å)	c (Å)	β (deg)	Volume (Å^3)
1 bar	9.328 (3)	13.578 (4)	6.592 (2)	106.60 (2)	800.1 (4)
0.63	9.105 (7)	13.307 (10)	6.454 (5)	106.38 (4)	750.3 (1)
1.0	9.035 (5)	13.219 (7)	6.419 (3)	106.34 (3)	735.8 (7)
1.7	8.940 (5)	13.114 (7)	6.369 (3)	106.50 (3)	715.9 (7)
2.14	8.852 (4)	12.972 (6)	6.310 (3)	106.54 (3)	694.6 (6)
2.8	8.823 (6)	12.902 (9)	6.273 (4)	106.49 (4)	684.6 (8)
3.2	8.801 (4)	12.859 (6)	6.258 (3)	106.64 (3)	678.6 (6)
3.4	8.794 (7)	12.814 (10)	6.237 (5)	106.67 (4)	673.3 (9)
4.35	8.772 (11)	12.728 (16)	6.179 (8)	106.87 (7)	660.2 (2)
5.56	8.763 (3)	12.542 (5)	6.137 (2)	107.07 (2)	644.8 (4)
6.52	8.723 (6)	12.423 (8)	6.079 (4)	107.18 (4)	629.4 (7)

parameters were approximately equal. Maximum possible errors can be by many times greater, however the probability of such errors is substantially reduced. By increasing the separation parameter $\Delta(1/d^2)$ for the considered reflections by 2–4 times, it was possible to obtain a much more detailed (comprehensive) set of calculated reflections (in the selected stick patterns), more adequate for the real diffraction picture (see [19, 20]). Nevertheless, the calculated realgar lattice parameters in this case kept within the limits of the errors. It should be noted that the identification of a monoclinic structure from the powder diagram is a rather difficult problem, especially if it is remembered that the unit cell of realgar contains four As_4S_4 molecules. The identification of an unknown structure from only small segments (figure 2) of the full powder diffraction pattern would have hardly been

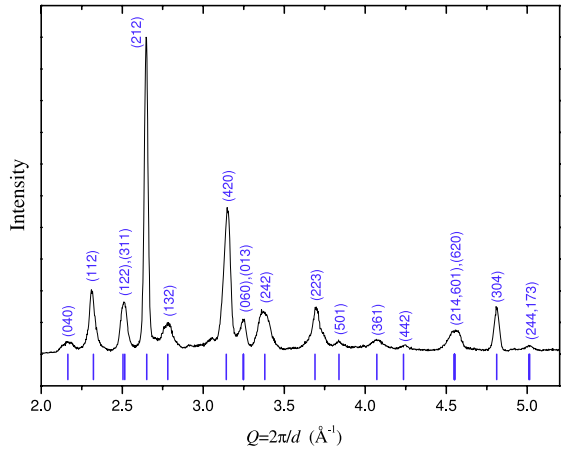

Figure 3. X-ray diffraction pattern of the new phase at $P = 7.46$ GPa. The indexing and stick pattern correspond to the orthorhombic structure.

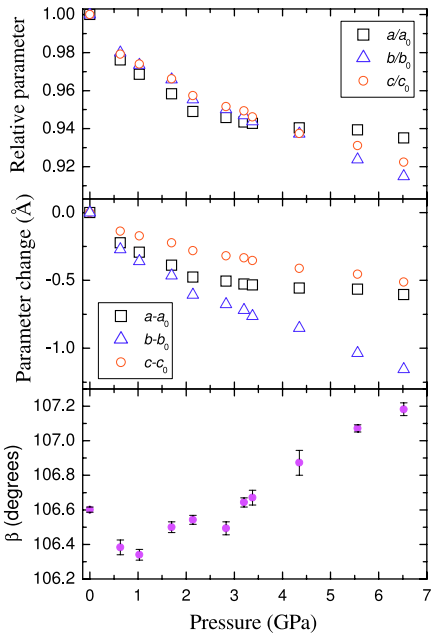

Figure 4. Pressure dependences of relative and absolute changes of the lattice parameters a, b and c, as well as the β angle for realgar. The uncertainties for a, b and c do not exceed the symbol sizes.

possible even using the analysis by the Rietveld refinement. Note that even some strong reflections for realgar are indexed differently in [19] and [20]. In addition, the variation of peak amplitudes in the diffraction patterns of realgar taken at normal pressure by different techniques (figures 1 and 2) differ slightly from each other in the common Q interval (with regard to the angle corrections for usual diffraction pattern and the detector corrections for the EDXD method). Nevertheless, comprehensive data on the initial structure of realgar and the corresponding powder diffraction pattern, as well as a sufficient number of observed reflections in the high pressure data, have enabled us to reliably trace the changes in the lattice parameters of realgar under pressure.

At pressures exceeding ≈7 GPa, the x-ray diffraction patterns changed considerably and became simpler (figure 3), which is indicative of a transition to a high pressure phase. The comparative analysis of strong reflections of the new phase permitted the suggestion that at high pressure a polymorphic transition to the orthorhombic phase, having a primitive unit cell and lattice parameters a, b, c close to those of a monoclinic phase, takes place. The results of the indexing of As_4S_4 at a pressure of 7.46 GPa in the orthorhombic singony are shown in table 3. The calculated parameters of a unit cell of the new phase for two experimental pressure points are given in table 4. Assuming that the number of As_4S_4 molecular units in the cell remains constant during this phase transition, we get the relative volume change $\Delta V/V = -6\%$. After pressure release, the structure of the samples was similar to that of realgar, i.e., the above transition was reversible. As the volume jump resulting from the transition is small and the transition is reversible, it can be concluded that the structure of the new phase remains a molecular one. The orthorhombic unit cell parameters, obtained from the indexing of the new phase, and the parameters of the initial monoclinic phase are related in the pressure-adjacent points by the correlations $a_{ort} \approx a_{mon}$ and $c_{ort} \approx c_{mon}$ with a discrepancy of about 2%. Considering the volume drop at the transition $\Delta V/V = -6\%$, we get $b_{ort} \approx b_{mon} \sin\beta$ with about the same 2% discrepancy. Thus, the spatial model of this transition can be thought of as the removal of a monoclinic distortion in the plane (010) of realgar and the formation of an orthorhombic structure with close unit cell parameters. In this case, the changes of a molecular coordinates in the planes (010) result in an additional compression of molecule positions along the y axis.

Table 3. Intensity, experimental and calculated interplanar distances, and hkl indices for the diffraction reflections of the new high pressure phase at $P = 7.46$ GPa in the approximation of the orthorhombic structure.

Relative intensity	d_{exp} (Å)	hkl	d_{calc} (Å)
11	2.898	040	2.903
36	2.716	112	2.705
30	2.503	311	2.498
		122	2.508
100	2.373	212	2.370
11	2.262	132	2.259
55	1.996	420	2.000
6	1.937	060	1.935
		013	1.934
25	1.862	242	1.859
11	1.700	223	1.703
1	1.638	501	1.637
3	1.543	361	1.543
1	1.482	442	1.483
7	1.380	620	1.380
		601	1.381
		214	1.381
6	1.306	304	1.306
1	1.254	173	1.253
		244	1.254

The compression of realgar can be analyzed in more detail. Figure 4 displays the relative and absolute lattice parameter changes with pressure. Up to a pressure of 4.5 GPa, the relative changes in the parameters a, b and c are close (figure 4(a)). A

Table 4. Lattice parameters of the new high pressure phase.

Pressure (GPa)	a (Å)	b (Å)	c (Å)	Volume (Å^3)
7.46	8.522 ± 0.004	11.611 ± 0.006	5.885 ± 0.003	582.3 ± 0.8
7.9	8.490 ± 0.004	11.581 ± 0.006	5.872 ± 0.003	577.3 ± 0.8

further increase in pressure leads to a discrepancy between the dependences, the lattice of realgar becoming more compressed along the $\boldsymbol{b}$ direction. In absolute values (figure 4(b)), the greatest change corresponds to b as well; the smallest change corresponds to c. In doing so, the b dependence noticeably deviates downwards with pressure. Note that the β angle mainly increase with pressure. Some decrease of β within 1 GPa can be explain for several reasons. First, it may be a regular dependence with pressure. It is more likely that this nonmonotonic $\beta(P)$ dependence is related to the polycrystalline state of the sample and, therefore, to possible changes in a field of shear stresses of individual crystallites with pressure changes. Such changes are especially irregular at the beginning stage of pressurizing, when the amorphous boron–epoxy resin mixture environment of the sample reaches the plastic regime of compression. It may be also important, that the realgar sample was preliminarily pressed from the powder to a tablet. In any case the observed irregularity of the $\beta(P)$ dependence can not significantly influence the further discussion and the final conclusions.

Changes in the parameters a, b and c under pressure can reasonably be linked to the peculiarities of the realgar structure (figure 5). Formally, the unit cell of realgar (figure 5) includes four molecules (for example, 1–4), positions of which are determined by positions of 8 atoms in one molecule and application of the $P2_1/n$ symmetry group operations for atoms of other 3 molecules. From the practical standpoint, the structure of realgar can be represented as alternate, of two types, corrugated molecular layers parallel to the $\boldsymbol{a}$ and $\boldsymbol{c}$ vectors and perpendicular to the $\boldsymbol{b}$ vector. In doing so, the bends in the layer correspond to the $\boldsymbol{a}$ direction, while along the $\boldsymbol{c}$ direction the molecules form linear chains. For example, the first layer is formed by molecules 1 and 2 (figure 5(a)) and by their translations along $\boldsymbol{a}$ and $\boldsymbol{c}$; the second layer is similarly formed by molecules 3 and 4. When considering the intermolecular interaction, it should be noted that the attraction between the molecules is associated with electrostatic orientational, induction, and dispersion forces, in which all atoms in the molecules are involved. The repulsion forces between the molecules are related to the overlapping of the electron shells of atoms in molecules, i.e., the repulsion forces are governed by the interaction of the nearest neighbor atoms in a molecular pair. Intermolecular pairs of the nearest atoms were analyzed in [8], and this analysis is easy to reproduce using a standard software package Diamond (Crystal Impact GbR). As in [8], distances of under 4 Å can reasonably be chosen as a criteria for the presence of intermolecular bonding for repulsion, since there is a gap in the 4 Å region for distances in the bar chart of interatomic distances; in this case, for As–As and As–S pairs these gaps extend towards smaller distances, as well. For molecule 4 (figure 5(a)), the intermolecular bonding is

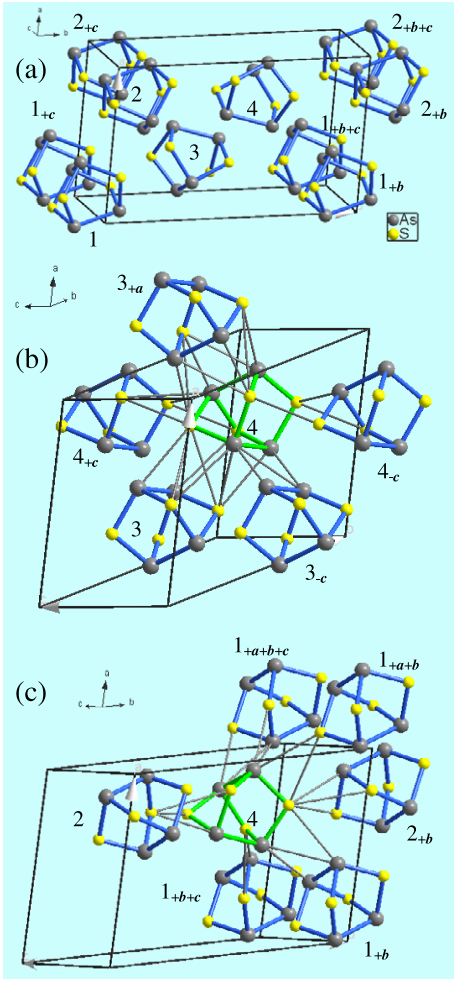

Figure 5. Elementary cell (a) and the structure of nearest neighbors for the molecule 4 in its own corrugated molecular layers parallel to the $\boldsymbol{a}$ and $\boldsymbol{c}$ (b) and in the corresponding nearest layers (c). The thick bonds correspond to the intramolecular ones, the thin bonds—to intermolecular for repulsion (see the text). Panels (a)–(c) have the same molecular numeration, where the low indices correspond to the translational vectors relative to the basis molecules 1–4.

presented in figures 5(b) and (c), respectively, for the proper corrugated layer of molecular 4 and for neighboring layers. The greatest number of intermolecular bonds is found in the proper corrugated layer (figure 5(b)), and the molecule has five neighbors. An additional molecule in the layer, designated in figure 5 as 3_{+a-c}, is found to be more remote due to the monoclinic distortion in the plane of the vectors $\boldsymbol{a}$ and $\boldsymbol{c}$. It is obvious that the least absolute compressibility of realgar along $\boldsymbol{c}$ is due to the fact that this is the only translation vector generating nearest neighbors (2 in number) for each molecule (in turn, such neighbors forms strict linear chains). Figure 5(c) explains why the most compressibility is observed

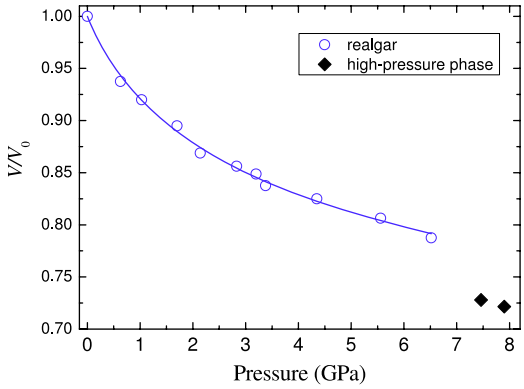

Figure 6. Pressure dependences of relative volume for realgar (open circles correspond to experimental points, the line—approximation) and the high pressure polymorph (diamonds) in the case of the suggested orthorhombic structure.

along $\boldsymbol{b}$. Whereas the molecule 4 strongly interacts with one nearest (010) molecular layer by repulsive forces via 5 bonds, interaction of this molecule with another nearest layer is weak and only via one bond. Clearly, the above description of the interaction between molecule 4 and its neighbors will be true for other molecules because of the symmetry of realgar. So, for each molecule there is a soft mode with respect to repulsion along $\boldsymbol{b}$, while in the planes parallel $\boldsymbol{a}$ and $\boldsymbol{c}$, the packing of molecules is relatively rigid.

From figure 5, possible stimuli for the high pressure phase transition discussed above can be described as well. A strong repulsive interaction of molecule 3 and 4 with the neighboring, but different corrugated layers (displaced relatively to each other by the translation $\boldsymbol{b}$) leads to an alignment of their positions along $\boldsymbol{b}$. At some moment, the monoclinic distortion in each of the corrugated layers is removed. As a result, every molecule in the layer becomes circled by six neighbors with a denser molecular packing in the layer. The nonequivalence of the orientations of molecule 3 and 4 (and their translations along $\boldsymbol{a}$ and $\boldsymbol{c}$) determines the orthorhombic symmetry of the packing in the layer. The same is true for molecule 1 and 2 and their common corrugated layer along $\boldsymbol{a}$ and $\boldsymbol{c}$. It is worth noting that in the framework of the described scenario, the formation of structures with hexagonal or trigonal symmetry is possible if a significant reorientation of molecules in the layer takes place. However, attempts to identify the picture in figure 3 in these singonies failed to produce valid results.

The pressure dependence of the unit cell of realgar $V = abc\sin\beta$ is shown in figure 6. The obtained experimental results $V(P)$ are well approximated (figure 6) by the Murnaghan equation corresponding to the linear dependence of the bulk modulus:

$$V = V_0\left(1 + P\frac{B_0'}{B_0}\right)^{-\frac{1}{B_0'}}, \qquad (2)$$

where B_0 is the bulk modulus at zero pressure and B_0' is its pressure derivative. The results of the corresponding fitting give the following values: $B_0 = 8.1 \pm 0.5$ GPa and $B_0' = 9.0 \pm 0.5$. It should be noted that a rough estimate of the bulk modulus of As_4S_4, made from the measurements of pressure and temperature dependences of the Raman frequencies [6], is too high. Correspondingly, more accurate current values of the bulk modulus of realgar make it possible to differentiate accurately between the phonon-excitation and the volume-driven contributions to the temperature derivatives of the phonon frequencies $d\omega/dT$ of realgar [6].

Table 5. Bulk modulus and its pressure derivative for some inorganic and simple organic molecular crystals.

Substance	B (GPa)	B'	Ref.
Realgar As_4S_4	8.1	9.0	Current work
As_4S_3	17	5.5	[21]
S_8	8.843	6.54	[22]
I_2	8.4	6.0	[22]
C_6Br_6	9.077	8.74	[23]
$C_{14}H_{10}$ anthracene	7.5	7.3	[23]
$C_{12}H_{18}$ hexamethyl-benzene	7.187	6.55	[23]
$C_{10}H_8$ naphthalene	6.727	7.13	[23]
$C_{18}H_{14}$ p-terpeny	6.015	7.7	[23]
$C_{14}H_8O_2$ anthraquene	9.245	8.32	[23]
$C_{13}H_{10}O$ benzophenone	7.306	8.18	[23]
$C_{14}H_{10}O$ anthrone	8.085	7.36	[23]

It is appropriate to compare the values of the bulk moduli and their derivatives for other molecular crystals (table 5). As can be seen, the values B_0 and B_0' obtained in this work for realgar fall in the range of values typical for this class of substances. The most outstanding of them is As_4S_3: despite being very close to realgar in composition and density; its bulk modulus is almost twice as large and its derivative is nearly twice as small as those for realgar. This is likely to be associated with a higher lattice symmetry of As_4S_3 [21]. Also worth noting are the large values of the bulk modulus derivatives B' of the molecular substances in the range from 6 to 9 (GPa). For many classes of substances, for example, most elementary substances, the B' values are usually smaller in the typical range from 2 to 5 (GPa) [24], although there is no general rule here and many non-molecular substances have large pressure derivatives B_0'. There are, however, natural explanations for large B_0' values for molecular substances. The intermolecular interactions are greatly influenced by the central interactions. To a first approximation, the latter can be appreciated through an effective central intermolecular interaction. For the case of the m–n power potential $U(V) = A/V^m - B/V^n$ (here, A, B, m, and n are constants), it is well known that the pressure derivative of bulk modulus is $B_0' = m + n + 2$ [25]. For the Lennard-Jones potential, $B_0' = 8$, which basically holds true for noble gases in the solid state [24]. Other molecular crystals have approximately the same pressure derivatives, although an increase in the molecule size is expected to result in an enhancement of the repulsive rigidity, i.e., in an increase of the m value. For example, for fullerite C_{60} $m \approx 14$ and $n = 3$ [26]. Indeed, for the fcc phase of C_{60} large derivatives $B_0' > 20$ are observed experimentally [27, 28].

Another aspect of the equation of state of realgar is associated with the linear pressure dependence of the bulk modulus. The condition $B_p' = \text{const}$ determines the

applicability of the Murnaghan equation (2) for the description of the equation of state. For symmetric cubic crystals with the Lennard-Jones central potential, B'_p rather rapidly decreases under compression (by 25% under a change of the volume $\Delta V/V \approx 0.2$) [29]. That is, for molecular crystals at $P \sim 0.5B_0$, a noticeable nonlinearity of the dependence $B(P)$ can already be observed. This effect is enhanced with a relative increase of rigidity for the repulsion potential (for the m–n potential, it is an increase in the m/n ratio) [29]. For example, in crystalline C_{60} the nonlinearity $B(P)$ is observed already at $P \sim 0.1B_0$ [28]. Another example is usual sulfur. Reference [24], along with the values listed in table 5 for orthorhombic S_8, gives $B_0 = 14.5$ GPa and $B'_0 = 7$, incidentally obtained in [30] in the study on high pressure phases. Both values are outside the range typical for molecular crystals. However, in [30] these values were obtained by using the Birch equation (corresponding also to the linear dependence $B(P)$ with good accuracy and, in fact, being very close to equation (2)) for the approximation of the four experimental points $V(P)$. From the graphic data in [30], it is seen that this approximation is inaccurate, apparently, because the condition $B'_p = \text{const}$ is not met. That is, B_0 and B'_0 for sulfur in [22] are likely to be more accurate. On the other hand, equation (2) gives a good approximation for realgar in the pressure range up to $P \sim 0.5B_0$. This may evidently be linked to a low symmetry of the realgar lattice and possible variation in the orientation of molecules in the cell. Changes of molecular orientations provide some additional molecular degrees of freedom for the relaxation of intermolecular stresses. In doing so, the intermolecular interaction turns out to be more complicated than a simple central interaction. This is directly evidenced by a different and nonlinear (in terms of the derivatives) behavior of the realgar unit cell parameters under pressure (figure 4), reflecting a change in the relative positions and orientations of molecules.

Thus, the obtained equation of state of realgar under pressure and pressure dependences of the realgar unit cell parameters are in good agreement with the crystallographic and chemical structure of realgar, which needs to be further confirmed by *ab initio* calculations. In this case, a change in the unit cell parameters is likely to be a precursor of the phase transition to a new molecular phase, observed under pressure. It will certainly be interesting to conduct a more detailed study under pressure of a closely related compound As_4S_3, whose equation of state [21] is somewhat anomalous for molecular crystals. Other phases of As_4S_4 are also of interest for comparative study.

Acknowledgments

The authors wish to thank R A Sadykov, Yu B Lebed, S G Lyapin, M V Kondrin and A G Sinyakov for technical assistance and useful discussions. The synchrotron radiation experiments were performed at the SPring-8 with the approval of the JASRI (project 2005B0040). The work has been supported by the Russian Foundation for Basic Research (07-02-01275 and 08-02-00014), by the Russian Science Support Foundation, and by the Programs of the Presidium of the RAS.

References

[1] Nalwa H S (ed) 2001 *Handbook of Advanced Electronic and Photonic Materials and Devices, Chalcogenide Glasses and Sol–Gel Materials* vol 5 (San Diego, CA: Academic)
[2] Kolobov A V (ed) 2003 *Photo-Induced Metastability in Amorphous Semiconductors* (Weinheim: Wiley–VCH)
[3] Lowe A J, Elliott S R and Greaves G N 1986 *Phil. Mag.* B **54** 483
[4] Feltz A 1983 *Amorphe und Glasartige Anorganische Festkörper* (Berlin: Academic)
[5] Brazhkin V V, Gavrilyuk A G, Lyapin A G, Timofeev Yu A, Katayama Y and Kohara S 2007 *Appl. Phys. Lett.* **91** 031912
[6] Zallen R and Slade M L 1978 *Phys. Rev.* B **10** 5775
[7] Chattopadhyay T, Werner A and v Schnering H G 1982 *J. Phys. Chem. Solids* **43** 277
[8] Ito T, Morimoto N and Sandanaga R 1952 *Acta Crystallogr.* **5** 775
[9] Hall H T 1966 The system Ag–Sb–S, Ag–As–S, and Ag–Bi–S: phase relations and mineralogical significance *PhD Thesis* Brown University, Providence, RI
[10] Roberts A C, Ansell H G and Bonardi M 1980 *Can. Mineral.* **18** 525
[11] Douglass D L, Shing C and Wang G 1992 *Am. Mineral.* **77** 1266
[12] Bonazzi P, Menchetti S, Pratesi G, Muniz-Miranda M and Sbrana G 1996 *Am. Mineral.* **81** 874
[13] Ballirano P and Maras A 2006 *Eur. J. Mineral.* **18** 589
[14] Kutolgu A 1976 *Z. Furanorg. Allg. Chem.* **419** 176
[15] Bonazzi P, Menchetti S and Pratesi G 1995 *Am. Mineral.* **80** 400
[16] Porter E J and Sheldrick G M 1972 *J. Chem. Soc., Dalton Trans.* **13** 1347
[17] Timofeeva N V, Vinogradova G Z, Feklichev E M, Apollonov V N, Kalashnikov Ya A, Dembovskii S A and Svintitskih V E 1972 *Sovremennye Problemy Phizicheskoi Khimii (Modern Problems of Physical Chemistry)* vol 6 (Moscow: Moscow State University) p 234 (in Russian)
[18] Hinze E and Lauterjung J 1990 *High Pressure Res.* **4** 324
[19] JCPDS-International Centre for Diffraction Data 2000 *PDF-2 Database* PDF number 41-1494
[20] JCPDS-International Centre for Diffraction Data 2000 *PDF-2 Database* PDF number 71-2434
[21] Chattopadhyay T, Werner A and v Schnering H G 1982 *J. Phys. Chem. Solids* **43** 919
[22] Vaidya S N and Kennedy G C 1972 *J. Phys. Chem. Solids* **33** 1377
[23] Vaidya S N and Kennedy G C 1971 *J. Chem. Phys.* **55** 987
[24] Knittle E 1995 *Mineral Physics and Crystallography: a Handbook of Physical Constants* ed T J Ahrens (Washington: AGU) p 98
[25] Aleksandrov I V, Goncharov A F, Zisman A N and Stishov S M 1987 *Sov. Phys.—JETP* **66** 384
[26] Zubov V I, Tretiakov N P, Sanchez J F and Caparica A A 1996 *Phys. Rev.* B **53** 12080
[27] Lundin A and Sandqvist B 1994 *Europhys. Lett.* **27** 463
[28] Yagafarov O F, Gromnitskaya E L, Lyapin A G, Brazhkin V V and Kondrin M V 2008 *J. Phys.: Conf. Ser.* **121** 022008
[29] Brazhkin V V and Lyapin A G 2002 *J. Phys.: Condens. Matter* **14** 10861
[30] Luo H and Ruoff A L 1993 *Phys. Rev.* B **48** 569